Computer Assisted Mechanics and Engineering Sciences, 14: 25–42, 2007.

MHD flow and heat transfer of a Bingham fluid in an eccentric annulus with the Hall effect

Mohamed E. Sayed-Ahmed[2], Hazem A. Attia[1,2]
[1] *Dept. of Mathematics, College of Science, Al-Qasseem University*
P.O. Box 237, Buraidah 81999, Saudi Arabia
[2] *Dept. of Engineering Mathematics and Physics, Faculty of Engineering*
Cairo University, El-Fayoum Branch, El-Fayoum-63111, Egypt

(Received December 15, 2004)

The steady laminar flow and heat transfer of an incompressible, electrically conducting, non-Newtonian Bingham fluid in an eccentric annulus are studied in the presence of an external uniform magnetic field. The inner cylinder is subject to a constant heat flux while the outer cylinder is adiabatic and, the viscous and Joule dissipations are taken into consideration. The governing momentum and energy equations are solved numerically using the finite difference approximations. The velocity, the temperature, the volumetric flow rate and the average Nusselt number are computed for various values of the physical parameters.

Nomenclature

$\mathbf{B}_o$	magnetic field
Br	Brinkman number
c_p	specific heat
D_h	hydraulic diameter of the duct
d	distance between centers of inner and outer cylinder
e	eccentricity
f_e	external magnetic force
Ha	Hartmann number
$\mathbf{J}$	current density
k	thermal conductivity
m	Hall parameter
Nu_a	average Nusselt number
p	pressure
Q	volumetric flow rate
$\bar{Q}$	dimensionless volumetric flow rate
R_1	radius of inner cylinder
R_2	radius of outer cylinder
Re	Reynolds number
Re_m	magnetic Reynolds number
S	radius ratio
T	temperature
$\bar{T}$	dimensionless temperature
$\bar{T}_m$	dimensionless fluid bulk mean temperature
$\bar{T}_w$	dimensionless temperature at the inner wall
$\bar{T}_{wa}$	dimensionless average wall temperature
u	axial velocity

u_a	average axial velocity
$\bar{u}$	dimensionless axial velocity
x, y, z	rectangular coordinates

Greek Symbols

β	Hall factor
θ	angle
ζ, η	bipolar coordinates
$\Delta\zeta$, $\Delta\eta$	uniform step sizes in bipolar coordinates
ζ_1, ζ_2	values of ζ at inner and outer surfaces of the annulus
μ	apparent viscosity
μ_o	plastic viscosity of Bingham fluid
$\bar{\mu}$	dimensionless apparent viscosity
ρ	density
σ	electric conductivity
τ_o	yield stress of Bingham fluid
τ_D	dimensionless yield stress of Bingham fluid

1. Introduction

Many of the fluids used for industrial purposes are non-Newtonian such as pastes, slurries, polymer solutions and melts, plastics, pulps and emulsions in every day chemical engineering practice. In particular, many of these materials exhibit shear-thinning behavior and in addition possess a yield stress below which the fluid either will not flow or will flow as an un-sheared plug (for low stress values the material will not deform, but beyond some critical value it flows as an inelastic non-Newtonian fluid). The Bingham model is one of the simplest models that describes materials with yield stress τ_0 and most widely model for the above materials. It is characterized by linear relation between shear stress and shear rate above the yield stress. The problem of the flow and heat transfer of non-Newtonian fluids has important applications in the flow of drilling fluids and cement slurries and in the design of coolant channels for power transformers, nuclear reactors, and the design of compact heat exchangers. Many researchers have studied the flow of a Bingham fluid in an eccentric annulus [4–6, 11–13]. Guckes [5] studied the flow of a power law and Bingham fluids in an eccentric annulus numerically using a finite difference technique. Further results were obtained for a power law fluid, Bingham material and Suterby fluids in a narrow eccentric annulus by Uner *et al.* [12] approximately by slit approximation method. Luo and Peden [6] carried out an analytical solution of power law and Bingham plastic fluids by representing the eccentric annulus as an infinite number of concentric annuli with variable outer radii. The analysis of the flow of a Bingham material in narrow eccentric annulus has been reported by Walton and Bittleston [13] using a perturbation technique and also a finite element method. A variational technique has been used for the evaluation of the characteristics of the flow of viscoplastic liquids in an eccentric annulus by Fortova *et al.* [4]. An analytical solution for small eccentricities has been presented by Szabo and Hassager [11] for Bingham fluids. They have verified the solution using a finite element method.

The problem of non-Newtonian fluids flow and heat transfer in the presence of an external magnetic field is of great interest in many engineering applications such as aerospace technology, turbomachinery, MHD power generators, MHD pumps, heat exchangers, underground cables, electronics, telecommunications, petroleum engineering and chemical engineering. Saranin [7] has examined a model problem of the flow of an electrically conducting, Newtonian fluid situated between coaxial cylinders heated to various temperatures and exposed to an external magnetic field with consideration given to the thermoelectric effects. Neglecting the Hall current, the problem of MHD flow and heat transfer of a Casson fluid in an eccentric annulus has been studied by [2, 8] numerically using a finite difference method.

In this paper, we study the effect of an external uniform magnetic field on the steady, laminar, fully developed flow and heat transfer of an electrically conducting Bingham fluid in an eccentric annulus. The Hall effect is considered while the induced magnetic field is neglected. The externally applied magnetic field is directed perpendicular to the cylinders and a uniform heat flux is applied to the inner cylinder while the outer cylinder is kept adiabatic. The momentum equation and the energy equation including the viscous and Joule dissipation terms are solved numerically using the method of finite differences. The influence of the model parameter, magnetic field and the Hall current on the velocity and temperature fields are reported.

2. Description of the problem

The geometry of the problem is shown in Fig. 1. R_1 and R_2 are the radii of the inner and outer cylinders respectively and "d" is the distance between the centers. The two horizontal cylinders have infinite extensions in the axial direction; z-direction. The annulus is characterized by two parameters namely the eccentricity "e" and the radius ratio "S" defined, respectively, by $e = d/(R_2 - R_1)$ and $S = R_1/R_2$. The fluid is assumed to be incompressible, electrically conducting, non-Newtonian with Bingham model. The fluid flows between the two cylinders in the axial direction with velocity u by the action of a constant pressure gradient. The flow is assumed to be laminar, steady and fully developed with uniform pressure over the cross section of the annulus. An external uniform magnetic field $\mathbf{B}_0$ is applied in the direction perpendicular to the flow in the y-direction and is assumed to be unaltered by considering very small magnetic Reynolds number ($Re_m \ll 1$) and then neglecting the induced magnetic field [3, 9]. Since the current trend for the application of MHD is towards a strong magnetic field, the influence of the electromagnetic force is noticeable [3]. Under these conditions, the Hall current is important and it has a marked effect on the magnitude and direction of the current density and consequently on the magnetic force term. Therefore, the Hall effect is taken into consideration. The inner cylinder is subject to a uniform heat flux q'' while the outer cylinder is adiabatic. From the geometry of the problem, it is clear that for all quantities are independent of the z-coordinate apart from the pressure gradient which is assumed to have a constant value.

The fluid motion is governed by the Navier–Stokes equation in the z-direction,

$$0 = -\frac{\mathrm{d}p}{\mathrm{d}z} + \frac{\partial}{\partial x}\left(\mu\frac{\partial u}{\partial x}\right) + \frac{\partial}{\partial y}\left(\mu\frac{\partial u}{\partial y}\right) + f_e\,, \qquad (1)$$

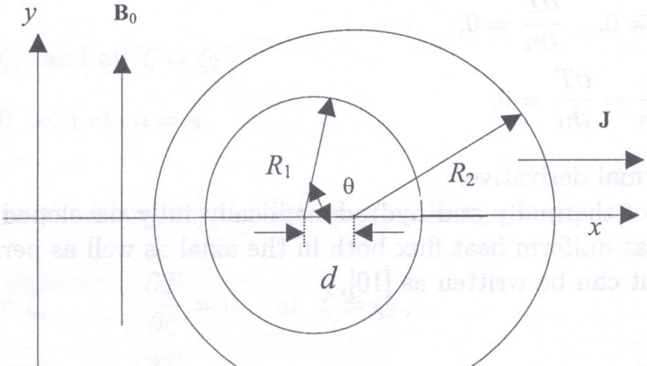

Fig. 1. The geometry of the eccentric annulus

where μ is the apparent viscosity of Bingham fluid and is given by [5],

$$\mu = \mu_0 + \frac{\tau_0}{\sqrt{\left(\frac{\partial u}{\partial x}\right)^2 + \left(\frac{\partial u}{\partial y}\right)^2}} \tag{2}$$

Here, μ_o is the plastic viscosity of the model and τ_0 is the yield value. f_e is the z-component of the electromagnetic Lorentz force given by $\mathbf{J} \times \mathbf{B}_o$, where $\mathbf{J}$ is the current density directed along the x-direction and is defined by the generalized Ohm's law [3, 9] in the form

$$\mathbf{J} = \sigma[\mathbf{v} \times \mathbf{B}_0 - \beta(\mathbf{J} \times \mathbf{B}_0)] \tag{3}$$

where σ is the electric conductivity of the fluid and β is the Hall factor [9]. Equation (3) may be solved in $\mathbf{J}$ to yield

$$\mathbf{J} \times \mathbf{B}_0 = -\frac{\sigma B_0^2}{1+m^2}(u\mathbf{k}) \tag{4}$$

where m is the Hall parameter and $m = \sigma \beta B_0$. Equation (4) tells that the current density $\mathbf{J}$ is proportional to the velocity u which preserves the symmetry conditions between the upper and lower halves of the annulus. Thus, the Navier–Stokes equation (1) reads

$$0 = -\frac{\partial p}{\partial z} + \frac{\partial}{\partial x}\left(\mu \frac{\partial u}{\partial x}\right) + \frac{\partial}{\partial y}\left(\mu \frac{\partial u}{\partial y}\right) - \frac{\sigma B_0^2}{1+m^2}\, u\,. \tag{5}$$

The energy equation with viscous and Joule dissipations is given by

$$\rho c_p u \frac{\partial T}{\partial z} = k\left(\frac{\partial^2 T}{\partial x^2} + \frac{\partial^2 T}{\partial y^2}\right) + \mu\left(\left(\frac{\partial u}{\partial x}\right)^2 + \left(\frac{\partial u}{\partial y}\right)^2\right) + \frac{\sigma B_0^2 u^2}{1+m^2}, \tag{6}$$

where T is the temperature of the fluid. ρ, c_p and k are, respectively, the density, the specific heat capacity and the thermal conductivity of the fluid. The last two terms in the right-hand-side of the above equation represent the viscous and Joule dissipations respectively.

The fluid motion is governed by the no-slip conditions at the inner and outer walls of the annulus and the symmetry conditions between the upper and lower halves of the annulus. The heat flux at the inner wall is given a constant value while its value is zero at the outer wall. These conditions are expressed as,

$$\begin{aligned} &\text{Inner wall:} && u = 0, \quad k\frac{\partial T}{\partial n} = \text{constant}, \\ &\text{Outer wall:} && u = 0, \quad \frac{\partial T}{\partial n} = 0, \\ &\text{Symmetry lines:} && \frac{\partial u}{\partial n} = \frac{\partial T}{\partial n} = 0, \end{aligned} \tag{7}$$

where $\frac{\partial}{\partial n}$ denotes the normal derivative.

Under the conditions of thermally and hydrodynamically fully developed state of laminar flow with heated surface kept at uniform heat flux both in the axial as well as peripheral directions, the axial temperature gradient can be written as [10],

$$\frac{\partial T}{\partial z} = \frac{2R_1 q''}{\rho c_p u_a \left(R_2^2 - R_1^2\right)}, \tag{8}$$

where u_a is the average velocity over the cross-section of the annulus.

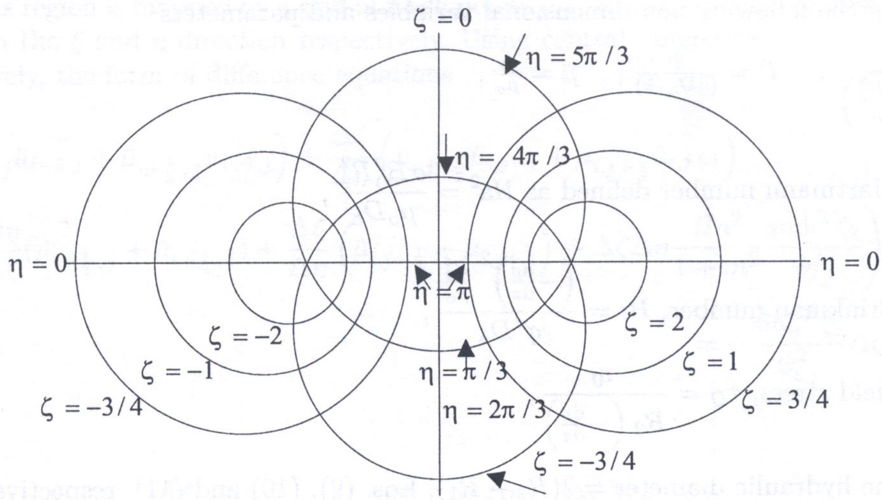

Fig. 2. Bipolar coordinate system

Using the Cartesian coordinate system in describing an eccentric annular geometry can be very cumbersome. Alternatively, the bipolar coordinate system shown in Fig. 2, that consists of two orthogonal systems of circles ζ and η is used which provides an excellent simplification [5]. Then, Eqs. (1) and (3) using the bipolar transformations take, respectively, the form

$$\left(\frac{\psi}{a_1}\right)^2\left(\frac{\partial}{\partial\zeta}\left(\mu\frac{\partial u}{\partial\zeta}\right)+\frac{\partial}{\partial\eta}\left(\mu\frac{\partial u}{\partial\eta}\right)\right)=\frac{\partial p}{\partial z}+\frac{\sigma B_0^2 u}{1+m^2}\,, \tag{9}$$

$$\rho c_p u\frac{\partial T}{\partial z}=k\left(\frac{\psi}{a_1}\right)^2\left(\frac{\partial^2 T}{\partial\zeta^2}+\frac{\partial^2 T}{\partial\eta^2}\right)+\mu\left(\frac{\psi}{a_1}\right)^2\left(\left(\frac{\partial u}{\partial\zeta}\right)^2+\left(\frac{\partial u}{\partial\eta}\right)^2\right)+\frac{\sigma B_0^2}{1+m^2}u^2. \tag{10}$$

where $\psi=\cosh\zeta-\cos\eta$ and $a_1=R_1\sinh\zeta_1=R_2\sinh\zeta_2$. Equation (2) becomes

$$\mu=\mu_o+\frac{\tau_0}{\left|\frac{\psi}{a_1}\sqrt{\left(\frac{\partial u}{\partial\zeta}\right)^2+\left(\frac{\partial u}{\partial\eta}\right)^2}\right|}\,. \tag{11}$$

The boundary conditions (7) for the velocity become

$$u=0\quad\text{at }\ \zeta=\zeta_1\ \text{ and at }\ \zeta=\zeta_2\,,$$
$$\frac{\partial u}{\partial\eta}=0\quad\text{at }\ \eta=0\ \text{ and at }\ \eta=\pi\,. \tag{12}$$

and for the temperature, the boundary conditions (7) take the form,

$$\frac{\partial T}{\partial\zeta}=\frac{a_1 q}{\psi k}\quad\text{at }\ \zeta=\zeta_1\,,\qquad\frac{\partial T}{\partial\zeta}=0\quad\text{at }\ \zeta=\zeta_2\,,$$
$$\frac{\partial T}{\partial\eta}=0\quad\text{at }\ \eta=0,\qquad\frac{\partial T}{\partial\eta}=0\quad\text{at }\ \eta=\pi\,. \tag{13}$$

By introducing the following non-dimensional variables and parameters:

$$\bar{u} = \frac{u}{\left(-\frac{\mathrm{d}p}{\mathrm{d}z}\frac{R_2^2}{\mu_o}\right)}, \quad \bar{T} = \frac{T}{(qD_h/k)}, \quad \bar{\mu} = \frac{\mu}{\mu_o},$$

Ha is the Hartmann number defined as $Ha^2 = \dfrac{\sigma B_0^2 R_2^2}{\mu_o D_h}$,

Br is the Brinkman number, $Br = \dfrac{\left(-\frac{\mathrm{d}p}{\mathrm{d}z}\right)^2 \frac{R_2^4}{\mu_o}}{q'' D_h}$,

τ_D is the yield stress, $\tau_D = \dfrac{\tau_0}{R_2\left(-\frac{\mathrm{d}p}{\mathrm{d}z}\right)}$,

where D_h is the hydraulic diameter $= 2(R_2 - R_1)$, Eqs. (9), (10) and (11), respectively, become

$$\frac{\partial}{\partial\zeta}\left(\bar{\mu}\frac{\partial\bar{u}}{\partial\zeta}\right) + \frac{\partial}{\partial\eta}\left(\bar{\mu}\frac{\partial\bar{u}}{\partial\eta}\right) - \frac{\sinh^2(\zeta_2)Ha^2}{\psi^2(1+m^2)}\bar{u} = -\frac{\sinh^2\zeta_2}{\psi^2}, \tag{14}$$

$$\frac{\partial^2\bar{T}}{\partial\zeta^2} + \frac{\partial^2\bar{T}}{\partial\eta^2} = \frac{\pi S\bar{u}\sinh^2\zeta_2}{(1-S)\bar{Q}\psi^2} - Br\,\bar{\mu}\left[\left(\frac{\partial\bar{u}}{\partial\zeta}\right)^2 + \left(\frac{\partial\bar{u}}{\partial\eta}\right)^2\right] - Br\,Ha^2\frac{\sinh^2\zeta_2}{\psi^2(1+m^2)}\bar{u}^2, \tag{15}$$

where $\bar{Q}$ is the volumetric flow rate given by

$$\bar{\mu} = 1 + \frac{\tau_D\sinh\zeta_2}{|\psi|\sqrt{\left(\frac{\partial\bar{u}}{\partial\zeta}\right)^2 + \left(\frac{\partial\bar{u}}{\partial\eta}\right)^2}} \tag{16}$$

and

$$\bar{Q} = 2\int_0^{\pi}\int_{\zeta_1}^{\zeta_2}\bar{u}\frac{\sinh^2\zeta_2}{\psi^2}\,\mathrm{d}\zeta\,\mathrm{d}\eta. \tag{17}$$

The boundary conditions (12) and (13) take, respectively, the non-dimensional form

$$\bar{u} = 0 \quad \text{at } \zeta = \zeta_1 \text{ and at } \zeta = \zeta_2, \qquad \frac{\partial\bar{u}}{\partial\eta} = 0 \quad \text{at } \eta = 0 \text{ and at } \eta = \pi, \tag{18}$$

and

$$\frac{\partial\bar{T}}{\partial\zeta} = \frac{\sinh\zeta_2}{2(\cosh\zeta_1 - \cos\eta)(1-S)} \quad \text{at } \zeta = \zeta_1, \qquad \frac{\partial\bar{T}}{\partial\zeta} = 0 \quad \text{at } \zeta = \zeta_2, \qquad \frac{\partial\bar{T}}{\partial\eta} = 0 \quad \text{at } \eta = 0 \text{ and at } \eta = \pi. \tag{19}$$

3. Numerical solution

The flow is described by Eq. (14) which in conjunction with the definition of $\bar{\mu}$ in Eq. (16) represents a non-linear partial differential equation which has to be solved numerically under the boundary conditions (18). Equation (15) with the boundary conditions (19) determine the temperature of the fluid. The values of the velocity component $\bar{u}$,obtained from the numerical solution of Eq. (14), when substituted in the right hand-side of the non-homogeneous energy equation (15), make it too difficult to solve analytically. Then Eqs. (14) and (15) are solved numerically with the appropriate boundary conditions using the method of finite differences.

The annulus region is mapped by a grid of mesh points $(\zeta_i\,,\,\eta_j)$. $\Delta\zeta$ and $\Delta\eta$ represent the uniform step lengths in the ξ and η direction respectively. Using central differences [1], Eqs. (14) and (15) take, respectively, the form of difference equations

$$\frac{\Delta\eta}{\Delta\zeta}\Big(\bar{\mu}_{i-\frac{1}{2},j}\bar{u}_{i-1,j}+\bar{\mu}_{i+\frac{1}{2},j}u_{i+1,j}\Big)+\frac{\Delta\zeta}{\Delta\eta}\Big(\bar{\mu}_{i,j-\frac{1}{2}}\bar{u}_{i,j-1}+\bar{\mu}_{i,j+\frac{1}{2}}\bar{u}_{i,j+1}\Big)$$
$$-\left(\frac{\Delta\eta}{\Delta\zeta}(\bar{\mu}_{i-\frac{1}{2},j}+\bar{\mu}_{i+\frac{1}{2},j})+\frac{\Delta\zeta}{\Delta\eta}\left(\bar{\mu}_{i,j-\frac{1}{2}}+\bar{\mu}_{i,j+\frac{1}{2}}\right)+\Delta\zeta\Delta\eta\frac{Ha^2}{1+m^2}\frac{\sinh^2\zeta_2}{\psi_{i,j}^2}\right)\bar{u}_{i,j}$$
$$=\frac{\sinh^2\zeta_2}{\psi_{i,j}^2}\Delta\zeta\Delta\eta \tag{20}$$

and

$$\frac{\Delta\eta}{\Delta\zeta}(\bar{T}_{i-1,j}+\bar{T}_{i+1,j})+\frac{\Delta\zeta}{\Delta\eta}(\bar{T}_{i,j-1}+\bar{T}_{i,j+1})-2\left(\frac{\Delta\eta}{\Delta\zeta}+\frac{\Delta\zeta}{\Delta\eta}\right)\bar{T}_{i,j}$$
$$=\Delta\zeta\Delta\eta\left(\left(\frac{\pi S}{(1-S)\bar{Q}}\bar{u}_{i,j}-Br\,\frac{Ha^2}{1+m^2}\bar{u}_{i,j}^2\right)\frac{\sinh^2\zeta_2}{\psi_{i,j}^2}-Br\,\bar{\mu}_{i,j}\left[\left(\frac{\partial\bar{u}}{\partial\zeta}\right)_{i,j}^2+\left(\frac{\partial\bar{u}}{\partial\eta}\right)_{i,j}^2\right]\right). \tag{21}$$

The problem of considering the apparent viscosity can be solved using an iterative procedure. The initial value for the viscosity is assumed at each grid point and then Eq. (20) with the differences form of the boundary condition (18), are used to calculate the unknown velocity values. Making use of these values, a new value of the apparent viscosity is obtained from the difference form of Eq. (16). The process is repeated up till the criteria of convergence

$$\left|\frac{\bar{u}_{i,j}^{\text{new}}-\bar{u}_{i,j}^{\text{old}}}{\bar{u}_{i,j}^{\text{new}}}\right|\le 10^{-4}$$

is satisfied. Then Eq. (21) with the difference form of the boundary condition (19) are used to solve for the temperature distribution. The system of linear equations is solved by the Successive Over-Relaxation method [1]. The convergence is achieved by taking 55×55 mesh points for both hydrodynamic and thermal parts. The average Nusselt number Nu_a at the inner wall is given by

$$Nu_a=\frac{1}{\bar{T}_{wa}-\bar{T}_m}\,, \tag{22}$$

where $\bar{T}_{wa}$ is the average temperature at the inner wall given in the form

$$\bar{T}_{wa}=\frac{\sinh\zeta_2}{\pi S}\int_0^{\pi}\frac{\bar{T}_w}{\cosh\zeta_1-\cos\eta}\,\mathrm{d}\eta, \tag{23}$$

and $\bar{T}_m$ is the mean fluid temperature given as

$$\bar{T}_m=\frac{2\sinh^2\zeta_2}{\bar{Q}}\int_0^{\pi}\int_{\zeta_1}^{\zeta_2}\frac{\bar{u}\bar{T}}{(\cosh\zeta-\cos\eta)^2}\,\mathrm{d}\zeta\mathrm{d}\eta. \tag{24}$$

The above defined integrals in Eqs. (17), (23) and (24) are evaluated numerically using Simpson's 1/3 rule [1]. Then the average Nusselt number can be estimated from Eq. (22).

4. Results and discussions

The distributions of the volumetric flow rate $\bar{Q}$ versus the eccentricity "e" are shown in Figs. 3, 4 and 5 (a,b,c) for $S = 0.3$, 0.5 and 0.7, respectively. The results are obtained for different values of the Hartmann number $Ha = 0,\ 1, 2, 3$, the Hall parameter $m = 0, 1, 2$, and the yield value $\tau_D = 0, 0.05, 0.1$. The study of these figures shows that, the volumetric flow rate $\bar{Q}$ increases with increasing the eccentricity "e" for all values of Ha, m and τ_D. However, increasing either Ha or τ_D reduces $\bar{Q}$ for every value of "e". It is also clear from the figures that the magnetic field has a marked effect on $\bar{Q}$ for larger values of "e" and smaller values of m. This is expected as the increment in "e" increases $\bar{Q}$ which, in turn, increases the damping magnetic force while increasing m decreases the damping magnetic force. Higher values of Ha reduce the influence of eccentricity on $\bar{Q}$ for all values of τ_D for $m = 0$ (neglecting the Hall current) and small value of radius ratio S. This effect becomes more pronounced for Newtonian fluids ($\tau_D = 0.0$). Increasing the value of the Hall parameter m increases $\bar{Q}$ for all values of Ha and τ_D. Higher values of m diminishes the effect of Hawhich becomes more apparent for larger values of τ_D. Figures 3–5 show that the increasing the radius ratio S decreases $\bar{Q}$ for all values of Ha, m and τ_D. The effect of the parameters Ha, m and τ_D on $\bar{Q}$ decreases greatly with increasing the radius ratio S.

The distributions of the centre velocity $\bar{u}_c$ with ϑ, (where ϑ is the polar angle of the central circle and is given by $\vartheta = \tan^{-1}((\sinh\zeta_1 \sin\eta)/(\cosh\zeta_1 \cos\eta - 1)))$ are shown in Figs. 6, 7 and 8 for $e = 0.2$, 0.4 and 0.6, respectively. The results are obtained for different values of the Hartmann number $Ha = 0,\ 1,\ 2,\ 3$, the Hall parameter $m = 0, 1, 3$, $\tau_D = 0, 0.05, 0.1$ for $S = 0.3$. It is clear from these figures that, the velocity $\bar{u}_c$ decreases with ϑ for all values of τ_D, m and Ha due to the effect of eccentricity. It is also observed that, increasing Ha decreases the velocity $\bar{u}_c$ for all values of τ_D. However, its effect is higher in the wide part of the annulus (near $\vartheta = 0$) than that in the narrow part (near $\vartheta = 180$). The value of $\bar{u}_c$ increases with increasing m. It is also observed that the effect of Ha on $\bar{u}_c$ becomes more pronounced for smaller values of the Hall parameter m. Increasing the eccentricity e increases the velocity in the wide part of the annulus and decreases it in the narrow part. Increasing "e" more stops completely the flow in the narrow part and consequently increases it more in the wide part.

Tables 1, 2 and 3 show the influence of the magnetic field and the Hall current on the average Nusselt number Nu_a for different values of "e" terms for the cases of Newtonian ($\tau_D = 0$) and non-Newtonian fluids ($\tau_D = 0.05$ and 0.1) and $S = 0.3, 0.5, 0.7$, respectively. The viscous and Joule dissipation terms are neglected ($Br = 0$). For all values of Ha, increasing "e" increases the volumetric flow rate $\bar{Q}$ due to increasing the velocity in the wide part of the annulus and decreases it in the narrow part and consequently reduces the temperature and the average Nu_a. Increasing Ha, although it decreases $\bar{Q}$, it increases Nu_a as a result of increasing the Joule dissipation. It is found that the effect of τ_D on Nu_a depends on the values of τ_D and the Hall parameter m. Increasing τ_D decreases Nu_a for all values of Ha, m, or S.

The effect of the Brinkman number Br on the average Nusselt number Nu_a for $S = 0.5$ and $\tau_D = 0.05$ is shown in Table 4 (a,b) for $m = 0$ and 1 and $Ha = 0, 1, 2$, respectively. In this case, the viscous and Joule dissipations are taken into consideration. It is found that increasing Br increases Nu_a for all values of e, m, and Ha.

5. Conclusions

In this paper, the steady MHD flow and heat transfer of an incompressible, electrically conducting, non-Newtonian Bingham fluid in an eccentric annulus were studied. Numerical solutions for the momentum equation and the energy equation including the viscous and Joule dissipations were obtained. The effect of the Hall current m on the flow and heat transfer characteristics was studied. Increasing the magnetic field decreases the velocity and the volumetric flow rate and its effect becomes more pronounced for high values of eccentricity or small values of the yield stress τ_D. Higher values of the magnetic field reduce the influence of eccentricity on the volumetric flow rate.

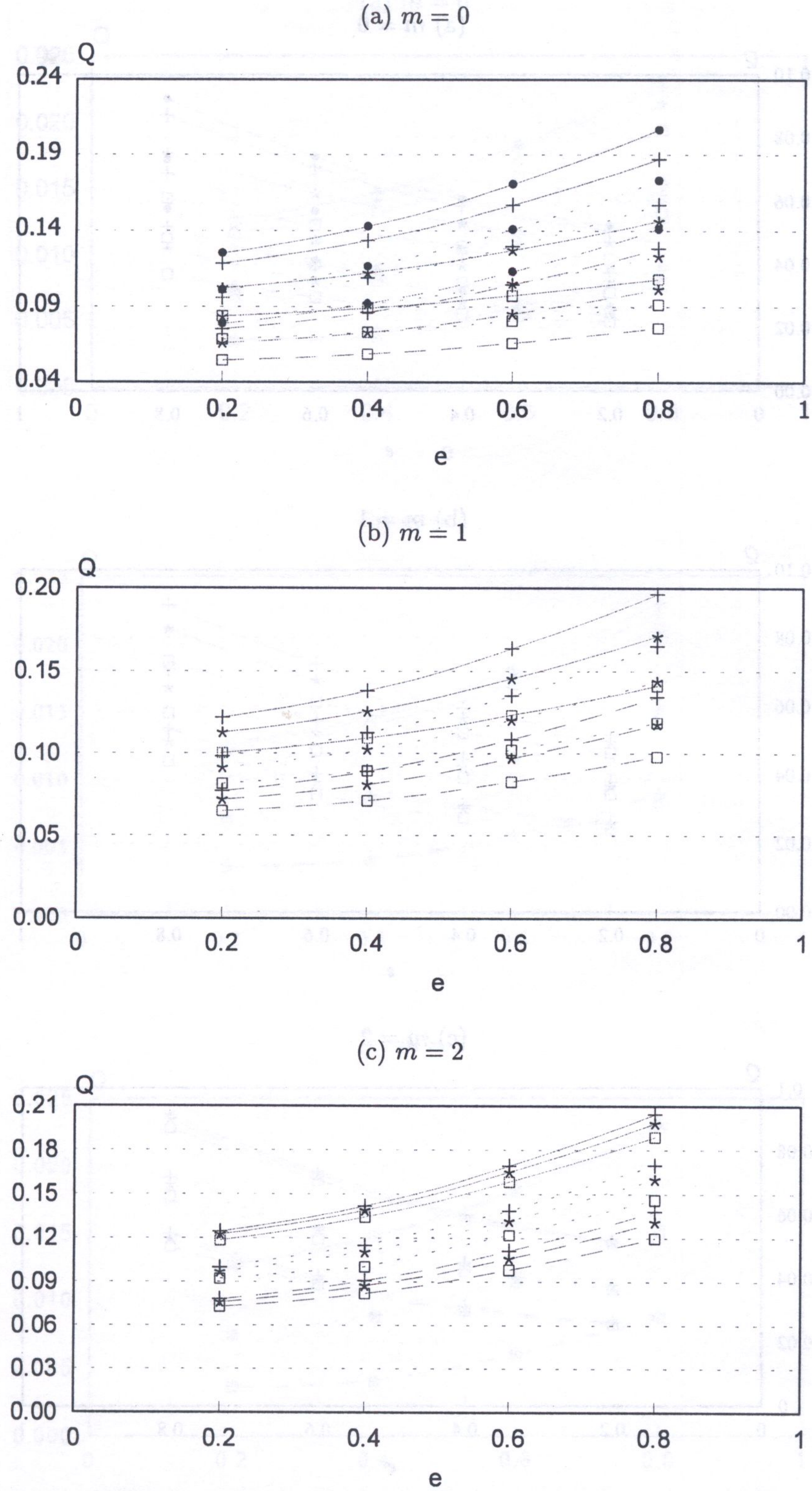

Fig. 3. The variation of the volumetric flow rate $\bar{Q}$ with the eccentricity e for $S = 0.3$; • $Ha = 0$, + $Ha = 1$, * $Ha = 2$, □ $Ha = 3$; —— $\tau_D = 0$, ······· $\tau_D = 0.025$, – – – $\tau_D = 0.05$

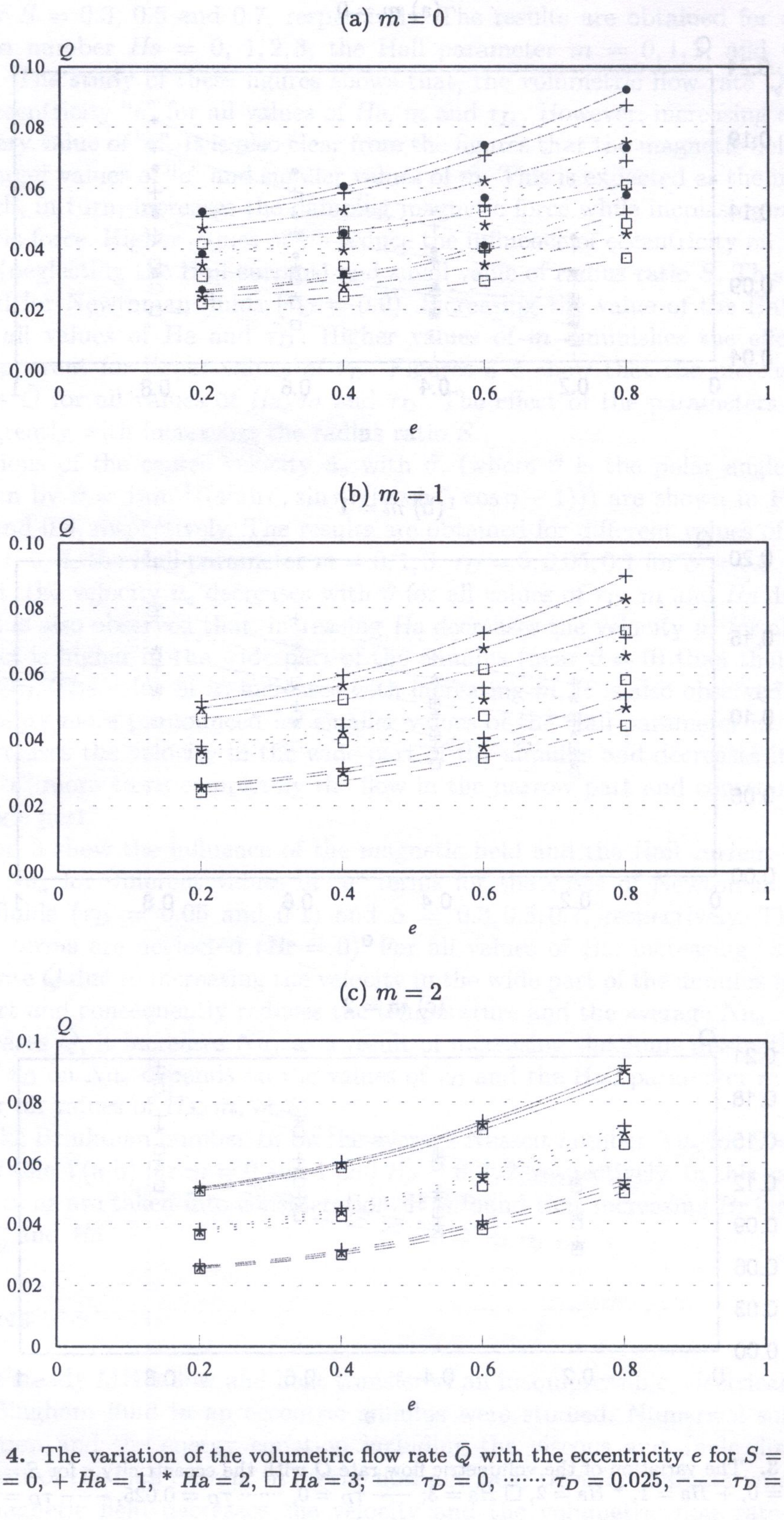

Fig. 4. The variation of the volumetric flow rate $\bar{Q}$ with the eccentricity e for $S = 0.5$; • $Ha = 0$, + $Ha = 1$, * $Ha = 2$, □ $Ha = 3$; —— $\tau_D = 0$, ······ $\tau_D = 0.025$, – – – $\tau_D = 0.05$

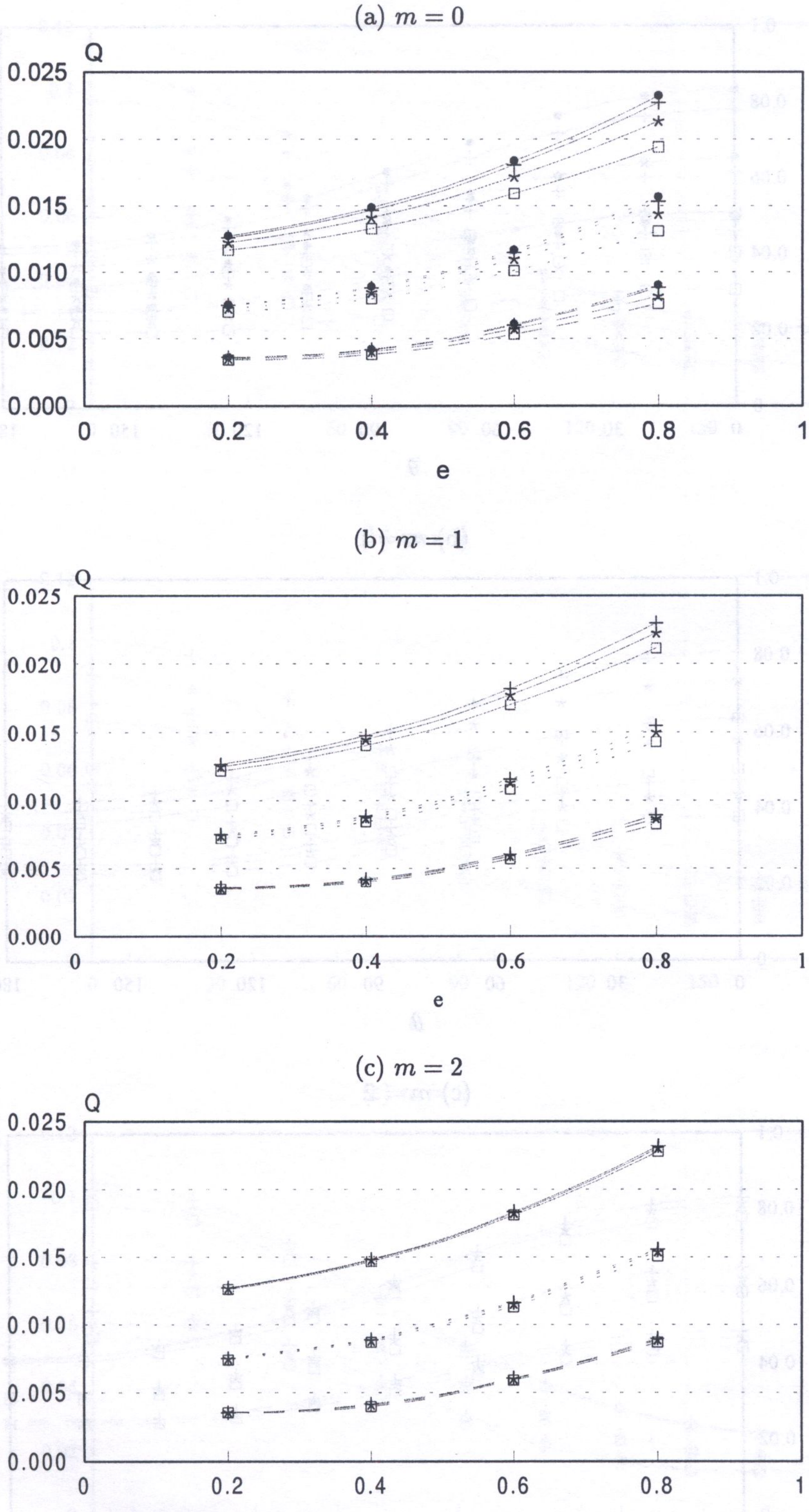

Fig. 5. The variation of the volumetric flow rate $\bar{Q}$ with the eccentricity e for $S = 0.7$; • $Ha = 0$, + $Ha = 1$, * $Ha = 2$, □ $Ha = 3$; —— $\tau_D = 0$, ······ $\tau_D = 0.025$, – – – $\tau_D = 0.05$

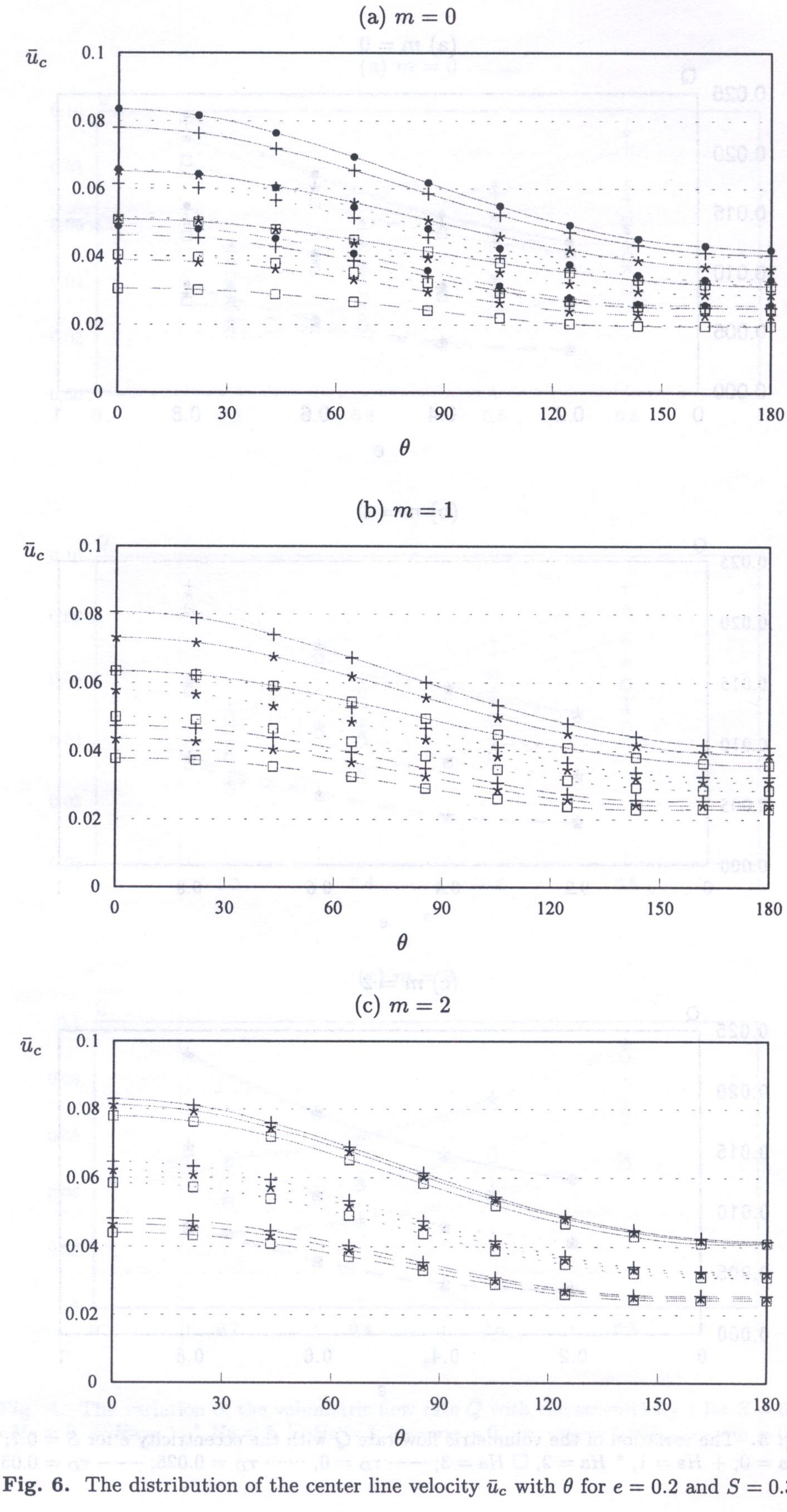

Fig. 6. The distribution of the center line velocity $\bar{u}_c$ with θ for $e = 0.2$ and $S = 0.3$

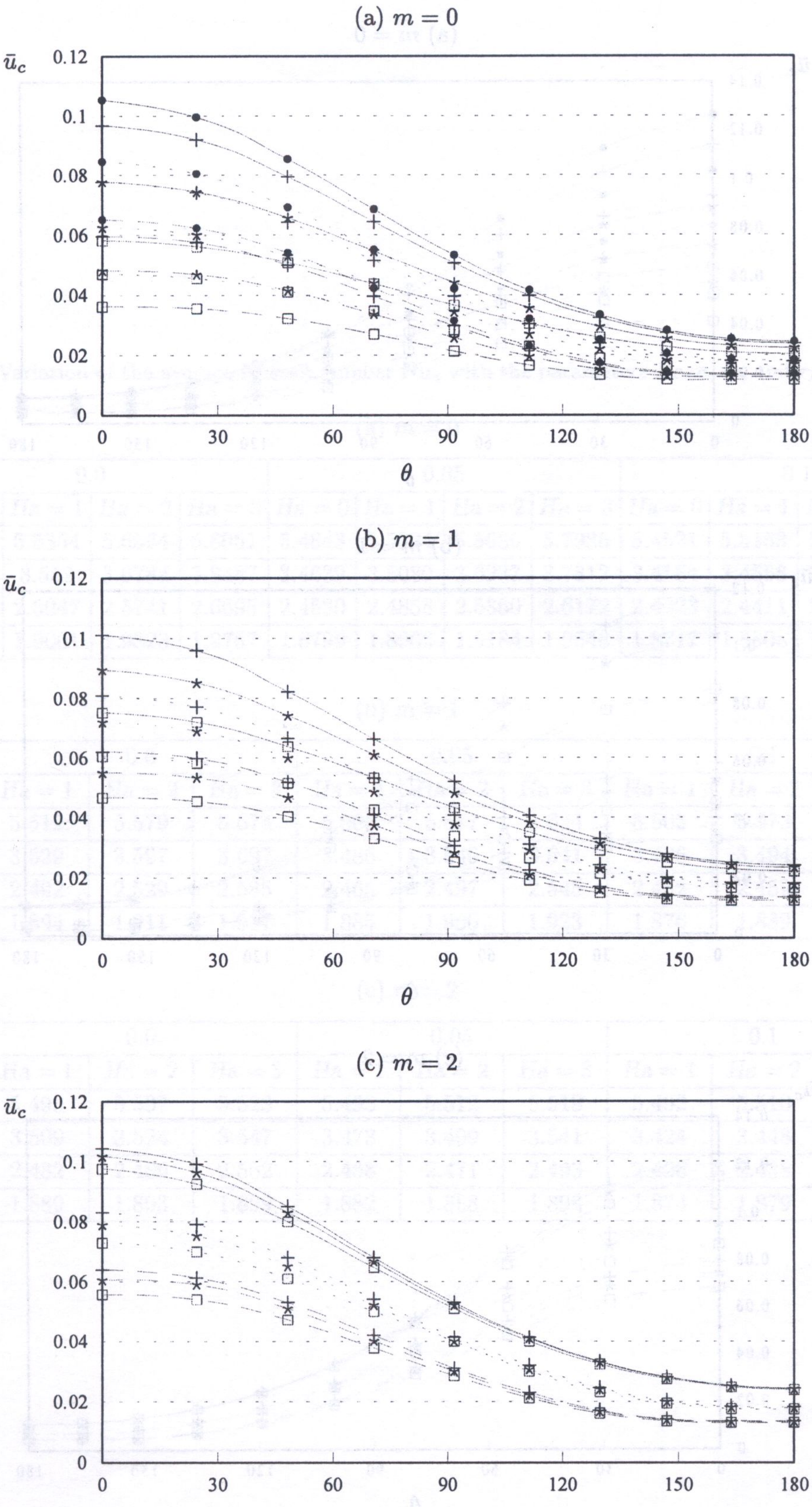

Fig. 7. The distribution of the center line velocity $\bar{u}_c$ with θ for $e = 0.4$ and $S = 0.3$

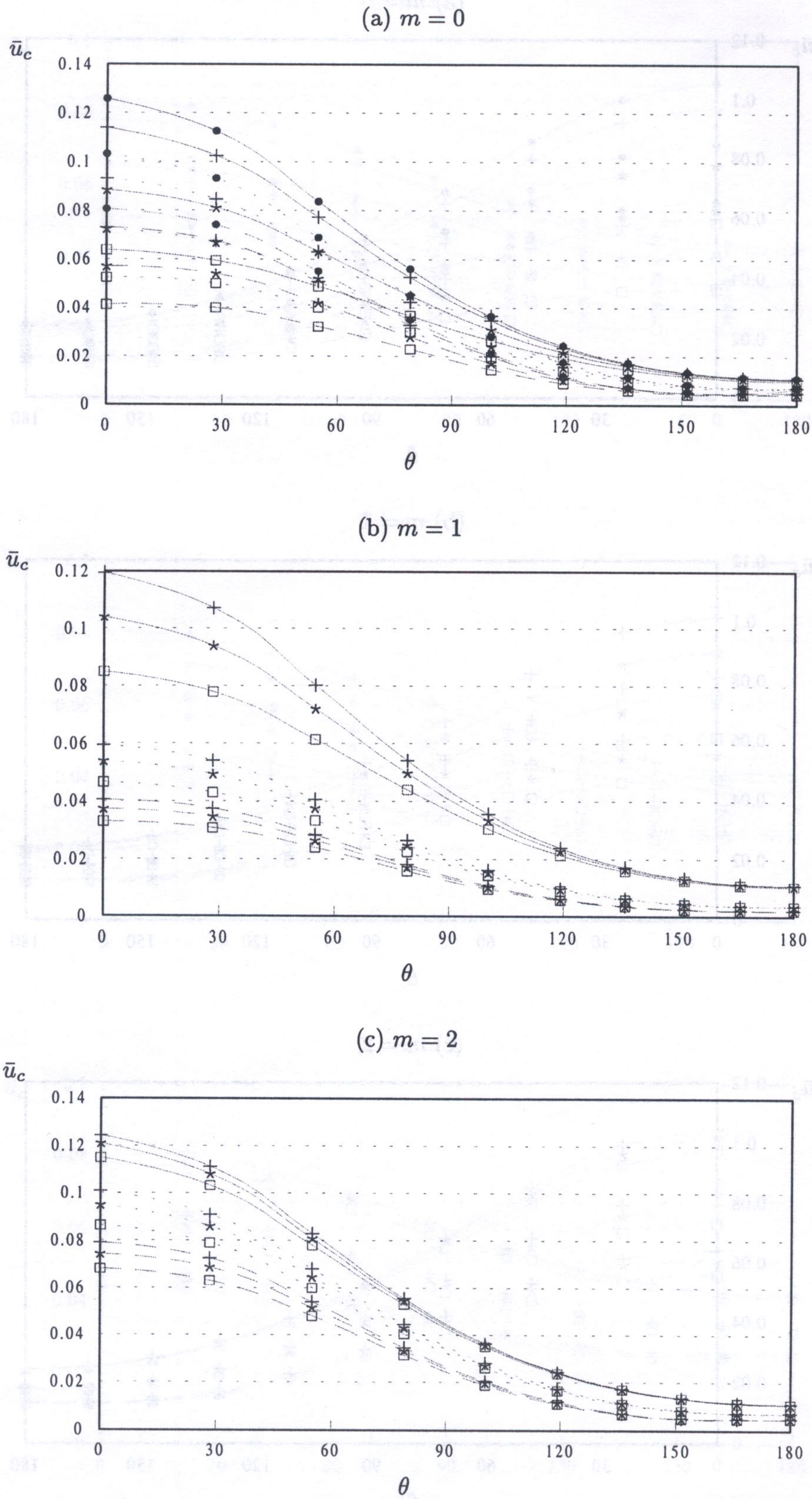

Fig. 8. The distribution of the center line velocity $\bar{u}_c$ with θ for $e = 0.6$ and $S = 0.3$

Table 1. Variation of the average Nusselt number Nu_a with the parameters Ha, e, m, and τ_D ($S = 0.3$)

(a) $m = 0$

$\tau_D =$	0.0				0.05				0.1			
e	$Ha = 0$	$Ha = 1$	$Ha = 2$	$Ha = 3$	$Ha = 0$	$Ha = 1$	$Ha = 2$	$Ha = 3$	$Ha = 0$	$Ha = 1$	$Ha = 2$	$Ha = 3$
0.2	5.4877	5.5354	5.6564	5.8051	5.4843	5.5324	5.5636	5.7986	5.4521	5.5163	5.5602	5.7842
0.4	3.5044	3.552	3.6784	3.8487	3.4639	3.5080	3.6237	3.7812	3.4164	3.4558	3.5609	3.7122
0.6	2.4790	2.5047	2.5741	2.6695	2.4530	2.4858	2.5360	2.6172	2.4223	2.4411	2.4915	2.5595
0.8	1.8881	1.9001	1.9323	1.9757	1.8799	1.8906	1.9184	1.9548	1.8717	1.8808	1.9035	1.9332

(b) $m = 1$

$\tau_D =$	0.0			0.05			0.1		
e	$Ha = 1$	$Ha = 2$	$Ha = 3$	$Ha = 1$	$Ha = 2$	$Ha = 3$	$Ha = 1$	$Ha = 2$	$Ha = 3$
0.2	5.512	5.579	5.674	5.508	5.577	5.634	5.503	5.573	5.636
0.4	3.529	3.597	3.697	3.486	3.549	3.641	3.436	3.494	3.577
0.6	2.492	2.529	2.585	2.465	2.497	2.545	2.432	2.459	2.499
0.8	1.894	1.911	1.937	1.885	1.900	1.923	1.876	1.889	1.907

(c) $m = 2$

$\tau_D =$	0.0			0.05			0.1		
e	$Ha = 1$	$Ha = 2$	$Ha = 3$	$Ha = 1$	$Ha = 2$	$Ha = 3$	$Ha = 1$	$Ha = 2$	$Ha = 3$
0.2	5.493	5.507	5.523	5.493	5.512	5.518	5.492	5.510	5.514
0.4	3.509	3.524	3.547	3.473	3.499	3.541	3.424	3.448	3.487
0.6	2.482	2.489	2.502	2.458	2.471	2.493	2.426	2.438	2.456
0.8	1.889	1.893	1.899	1.882	1.888	1.898	1.874	1.879	1.887

Table 2. Variation of the average Nusselt number Nu_a with the parameters Ha, e, m, and τ_D ($S = 0.5$)

(a) $m = 0$

$\tau_D =$	0.0				0.05				0.1			
e	$Ha = 0$	$Ha = 1$	$Ha = 2$	$Ha = 3$	$Ha = 0$	$Ha = 1$	$Ha = 2$	$Ha = 3$	$Ha = 0$	$Ha = 1$	$Ha = 2$	$Ha = 3$
0.2	3.217	3.254	3.358	3.511	3.105	3.146	3.244	3.387	3.089	3.143	3.242	3.373
0.4	1.552	1.573	1.6336	1.725	1.462	1.480	1.530	1.605	1.374	1.389	1.429	1.489
0.6	1.004	1.014	1.043	1.086	0.964	0.972	0.994	1.027	0.919	0.924	0.941	0.964
0.8	0.751	0.756	0.770	0.791	0.736	0.750	0.751	0.767	0.712	0.723	0.732	0.744

(b) $m = 1$

$\tau_D =$	0.0			0.05			0.1		
e	$Ha = 1$	$Ha = 2$	$Ha = 3$	$Ha = 1$	$Ha = 2$	$Ha = 3$	$Ha = 1$	$Ha = 2$	$Ha = 3$
0.2	3.235	3.289	3.375	3.124	3.175	3.258	3.118	3.167	3.245
0.4	1.563	1.594	1.643	1.471	1.497	1.538	1.382	1.403	1.435
0.6	1.009	1.024	1.048	0.968	0.980	0.998	0.921	0.930	0.944
0.8	0.753	0.761	0.773	0.738	0.744	0.753	0.722	0.735	0.733

(c) $m = 2$

$\tau_D =$	0.0			0.05			0.1		
e	$Ha = 1$	$Ha = 2$	$Ha = 3$	$Ha = 1$	$Ha = 2$	$Ha = 3$	$Ha = 1$	$Ha = 2$	$Ha = 3$
0.2	3.220	3.232	3.250	3.112	3.135	3.169	3.103	3.131	3.164
0.4	1.554	1.561	1.571	1.466	1.476	1.494	1.377	1.386	1.400
0.6	1.005	1.008	1.013	0.966	0.970	0.978	0.920	0.923	0.929
0.8	0.751	0.753	0.755	0.737	0.739	0.743	0.721	0.723	0.725

Table 3. Variation of the average Nusselt number Nu_a with the parameters Ha, e, m, and τ_D ($S = 0.7$)

(a) $m = 0$

$\tau_D =$	0.0				0.05				0.1			
e	$Ha = 0$	$Ha = 1$	$Ha = 2$	$Ha = 3$	$Ha = 0$	$Ha = 1$	$Ha = 2$	$Ha = 3$	$Ha = 0$	$Ha = 1$	$Ha = 2$	$Ha = 3$
0.2	1.285	1.295	1.324	1.372	1.120	1.128	1.151	1.189	1.117	1.122	1.146	1.165
0.4	0.477	0.480	0.490	0.506	0.340	0.402	0.408	0.419	0.332	0.333	0.337	0.343
0.6	0.293	0.294	0.299	0.307	0.259	0.256	0.263	0.267	0.225	0.226	0.227	0.229
0.8	0.219	0.220	0.223	0.226	0.205	0.206	0.207	0.210	0.192	0.192	0.197	0.195

(b) $m = 1$

$\tau_D =$	0.0			0.05			0.1		
E	$Ha = 1$	$Ha = 2$	$Ha = 3$	$Ha = 1$	$Ha = 2$	$Ha = 3$	$Ha = 1$	$Ha = 2$	$Ha = 3$
0.2	1.290	1.305	1.329	1.124	1.136	1.159	1.165	1.047	1.209
0.4	0.478	0.483	0.492	0.401	0.404	0.409	0.333	0.335	0.338
0.6	0.294	0.296	0.300	0.259	0.261	0.263	0.225	0.226	0.227
0.8	0.220	0.221	0.223	0.205	0.206	0.208	0.192	0.193	0.194

(c) $m = 2$

$\tau_D =$	0.0			0.05			0.1		
e	$Ha = 1$	$Ha = 2$	$Ha = 3$	$Ha = 1$	$Ha = 2$	$Ha = 3$	$Ha = 1$	$Ha = 2$	$Ha = 3$
0.2	1.286	1.289	1.294	1.121	1.126	1.134	1.191	1.167	1.175
0.4	0.477	0.478	0.480	0.400	0.401	0.404	0.332	0.333	0.334
0.6	0.293	0.293	0.294	0.259	0.260	0.261	0.225	0.226	0.226
0.8	0.219	0.220	0.220	0.205	0.206	0.206	0.192	0.192	0.193

Table 4. The effect of the parameters Br, Ha, e, and m on the average Nusselt number Nu_a for $S = 0.5$ and $\tau_D = 0.05$

(a) $m = 0$

$Ha =$	0			1			2		
e	$Br = 0$	1	2	$Br = 0$	1	2	$Br = 0$	1	2
0.2	3.105	3.129	3.152	3.146	3.165	3.188	3.244	3.265	3.286
0.4	1.462	1.481	1.501	1.480	1.498	1.518	1.530	1.548	1.566
0.6	0.964	0.984	1.004	0.972	0.991	1.010	0.994	1.011	1.029
0.8	0.736	0.758	0.782	0.750	0.761	0.784	0.751	0.770	0.790

(b) $m = 1$

$Ha =$	0			1			2		
e	$Br = 0$	1	2	$Br = 0$	1	2	$Br = 0$	1	2
0.2	3.105	3.129	3.152	3.146	3.147	3.171	3.165	3.198	3.220
0.4	1.462	1.481	1.501	1.480	1.490	1.510	1.498	1.516	1.534
0.6	0.964	0.984	1.004	0.972	0.987	1.007	0.991	0.998	1.017
0.8	0.736	0.758	0.782	0.750	0.760	0.783	0.761	0.764	0.786

Increasing the magnetic field increases the average Nusselt number Nu_a for an eccentric annulus. Increasing the Hall parameter m increases both of the velocity and the volumetric flow rate and decreases the average Nusselt number. The effect of the viscous and Joule dissipations on Nu_a is more pronounced for high values of eccentricity or small values of τ_D . Also, the effect of the magnetic field Ha on the flow and heat transfer characteristics is more pronounced for smaller values of the Hall current m.

REFERENCES

[1] H.M. Antia. *Numerical Methods for Scientists and Engineers.* Tata McGraw–Hill, New Delhi, 1991.

[2] A.M. Ateia, M.E. Sayed, H.H.S. El-Din. Magnetohydrodynamic flow and heat transfer of a Casson in an eccentric annulus. *Al-Azhar Engineering 7th International Conference, Cairo, Egypt*, April 7–10, 2003, CD Code M04/01.

[3] K. Cramer, S. Pai. *Magnetofluid Dynamics for Engineers and Applied Physicists.* McGraw–Hill, 1973.

[4] M. Fortova, M. Buchtelova, J. David. The axial laminar flow of a viscoplastic liquid in an eccentric annulus-a new approximate formula. *Acta Techn., CSAV*, **37**: 305–316, 1992.

[5] T.L. Guckes. Laminar flow of non-Newtonian fluids in an eccentric annulus. *Trans. ASME, J. Engrg. Industry*, **97**: 498–506, 1975.

[6] Y. Luo, J.M. Peden. Flow of non-Newtonian fluids through eccentric annuli. *SPE Producting Engineering*, **289**: 91–96, 1990.

[7] V.A. Saranin. Thermomagnetohydrodynamic motion of a melt in the gap between coaxial cylinders. *Magnetohydrodynamics*, **25**(1): 111–113, 1989.

[8] M.E. Sayed-Ahmed, H.A. Attia. Magnetohydrodynamic flow and heat transfer of a non-Newtonian fluid in an eccentric annulus. *Can. J. Phys.*, **76**: 391–401, 1998.

[9] G.W. Sutten, A. Sherman. *Engineering Magnetohydrodynamics.* McGraw–Hill, 1965.

[10] K. Suzuki, J.S. Szmyd, H. Ohtsuka. Laminar forced convection heat transfer in eccentric annuli. *Heat Transfer Jap. Res.*, **20**: 169–183, 1991.

[11] P. Szabo, O. Hassager. Flow of viscoplastic fluids in eccentric annular geometries. *J. Non-Newtonian Fluid*, **45**(2): 149–169, 1992.

[12] D. Uner, C. Ozgen, I. Tosun. An approximate solution for non-Newtonian flow in eccentric annuli. *Ind. Eng. Chem. Res.*, **27**: 678–701, 1988.

[13] I.C. Walton, S.H. Bittleston. The axial flow of a Bingham plastic in a narrow eccentric annulus. *J. Fluid Mech.*, **222**: 39–60, 1991.